

Article

Penrose Scattering in Quantum Vacuum

José Tito Mendonça 

GoLP/IPFN, Instituto Superior Técnico, Universidade de Lisboa, Av. Rovisco Pais 1, 1049-001 Lisboa, Portugal; titomend@tecnico.ulisboa.pt

Abstract: This paper considers the scattering of a probe laser pulse by an intense light spring in a QED vacuum. This new scattering configuration can be seen as the vacuum equivalent to the process originally associated with the scattering of light by a rotating black hole, which is usually called Penrose superradiance. Here, the rotating object is an intense laser beam containing two different components of orbital angular momentum. Due to these two components having slightly different frequencies, the energy profile of the intense laser beam rotates with an angular velocity that depends on the frequency difference. The nonlinear properties of a quantum vacuum are described by a first-order Euler–Heisenberg Lagrangian. It is shown that in such a configuration, nonlinear photon–photon coupling leads to scattered radiation with frequency shift and angular dispersion. These two distinct properties, of frequency and propagation direction, could eventually be favorable for possible experimental observations. In principle, this new scattering configuration can also be reproduced in a nonlinear optical medium.

Keywords: laser QED; scattering; nonlinear quantum vacuum

1. Introduction

The recent development of intense laser systems at the peta-watt level [1] opens the opportunity for a possible exploration of the quantum vacuum and its nonlinear optical properties. This has been discussed in several recent review papers (see, for instance, [2–4]). Many different physical geometries have been proposed for possible experiments with intense lasers in vacuum, especially those associated with photon–photon scattering, vacuum birefringence, four-wave mixing, photon reflection and acceleration, among others [5–9].

Most of these processes take place with moderately high electromagnetic radiation, not involving the creation of real electron–positron pairs, but simply the excitation of virtual pairs which can be seen as the components of a virtual plasma state. This state can be excited using field amplitudes that are very large when compared with common laser beams but stay well below the critical field [10], which is known as the *Schwinger field*. Vacuum optical processes in this moderately high regime can be described with the lowest order Heisenberg–Euler Lagrangian theory [11,12].

Due to the smallness of such vacuum quantum effects, several strategies have been proposed to increase these effects. Recent proposals include the photon–photon scattering of high-harmonic laser pulses and vacuum superradiance [13,14]. Here, we propose another possible configuration, which is directly inspired by traditional optical experiments using rotating mirrors, and that more recently was recreated in a gravitational context. This new context was first explored by Penrose [15], Zeldovich [16] and others as a way to extract energy from a rotating black hole, and it is sometimes called *Penrose superradiance* [17,18]. Recent observations of similar phenomena were claimed in nonlinear optics [19], in acoustics [20], and in hydrodynamics [21].

In previous papers, it was shown that vortex structures containing two or more internal modes with different frequency and helicity, called *light springs*, can be used for particle acceleration in plasmas [22,23]. Although somewhat surprising, the name "light spring" becomes obvious near a plasma cutoff when these optical structures behave like



Citation: Mendonça, J.T. Penrose Scattering in Quantum Vacuum. *Photonics* **2024**, *11*, 448. <https://doi.org/10.3390/photonics11050448>

Received: 15 April 2024

Revised: 6 May 2024

Accepted: 9 May 2024

Published: 10 May 2024



Copyright: © 2024 by the author. Licensee MDPI, Basel, Switzerland. This article is an open access article distributed under the terms and conditions of the Creative Commons Attribution (CC BY) license (<https://creativecommons.org/licenses/by/4.0/>).

a mechanical spring [24]. Here, we consider the possible use of similar structures in a pure vacuum. The energy density of such structures rotates around the propagation direction with an angular velocity that depends on the frequency difference of their internal modes. At high intensities, they can be used as a nonlinear scattering object for a probe beam propagating in the perpendicular direction. Here, we study the corresponding scattering process.

We describe the vacuum properties using the Euler–Heisenberg Lagrangian. The optical nonlinearity associated with an intense light spring is described in Section 2. The nonlinear quantum currents resulting from the interaction of this structure with a probe beam are described in Sections 3, and the properties of the scattered radiation resulting from this interaction are detailed in Section 4. The field amplitude, frequency and wavevector spectrum of the scattered radiation are given, and simple order of magnitude estimates are established. Finally, in Section 5, we state some conclusions.

2. Light Spring in Vacuum

We consider an intense laser pulse propagating in vacuum with orbital angular momentum (OAM). We assume that the pulse propagates along some arbitrary z -direction, and it is made of a superposition of two OAM modes, with different frequencies ω_1 and ω_2 , and different helicity characterized by the topological charges, or poloidal quantum numbers, ℓ_1 and ℓ_2 . This pulse configuration is sometimes called a light spring [23,25]. Using cylindrical coordinates, $\mathbf{r} \equiv (r, \theta, z)$, we can write the total electric field of the pulse as

$$\mathbf{E}_0(\mathbf{r}, t) = \sum_{\nu=1,2} \mathbf{E}_\nu F_\nu(r, \theta) \exp(ik_\nu z - i\omega_\nu t) + c.c., \quad (1)$$

where $\nu = 1, 2$ represent the two different helicity components. The transverse beam profile of each component is described by a *Laguerre–Gauss* function $F_\nu(r, \theta)$, and each value of ν represents two quantum numbers (p, ℓ) , where p characterizes the number of zeros in the radial direction, and ℓ defines the poloidal mode structure, as given by

$$F_\nu(r, \theta) = C_{p\ell} X^{|\ell|/2} L_p^{|\ell|}(X) \exp\left(i\ell_\nu \theta - \frac{X}{2} + i\varphi_G\right). \quad (2)$$

Here, L_p^ℓ are the Laguerre–Gauss functions of the dimensionless variable $X = r^2/w^2$, where the laser beam waist w slowly varies in the z direction. Due to propagation in vacuum, we necessarily have $k_\nu = \omega_\nu/c$. In this expression, we have included the *Guoy phase*, which is defined as

$$\varphi_G = (1 + 2p + |\ell|) \arctan(z/L_R), \quad (3)$$

where L_R is the *Rayleigh length*, defining the size of the focal region. This phase only plays a minor role in the present problem and can be ignored. The light spring intensity is determined by the following expression

$$|E_0|^2 = \sum_{\nu=1,2} |\mathbf{E}_\nu|^2 F_\nu(r)^2 + 2(\mathbf{E}_1 \cdot \mathbf{E}_2) F_1(r) F_2(r) \exp(\Delta k z + \Delta \ell \theta - \Delta \omega t), \quad (4)$$

where we have used the notation $F_\nu(r) = F_\nu(r, \theta) \exp(-i\ell\theta)$ and defined the differences

$$\Delta \ell = \ell_1 - \ell_2, \quad \Delta \omega = \omega_1 - \omega_2, \quad \Delta k = \Delta \omega / c, \quad (5)$$

between the two internal modes of the light spring. This expression is very interesting because it shows that the maximum intensity of the light spring follows a helical curve defined by [23]

$$\theta(z, t) = (z - ct) \frac{\Delta k}{\Delta \ell} \equiv (z - ct) \frac{(\omega_1 - \omega_2)}{c(\ell_1 - \ell_2)}, \quad (6)$$

For a given scattering position, $z = \text{constant}$, it therefore defines the angular rotation of a purely electromagnetic object moving in vacuum. Of particular interest for experimental purposes is the case where $\Delta l \simeq 1 \ll \ell_v$ and $\Delta\omega \ll \omega_v$, such that the radial field distributions of the two OAM modes nearly superpose. An intense light spring can then locally excite electron–positron (e-p) virtual states, thus leading to the scattering of a probe pulse propagating in a perpendicular direction. The geometry of our problem is represented in Figure 1.

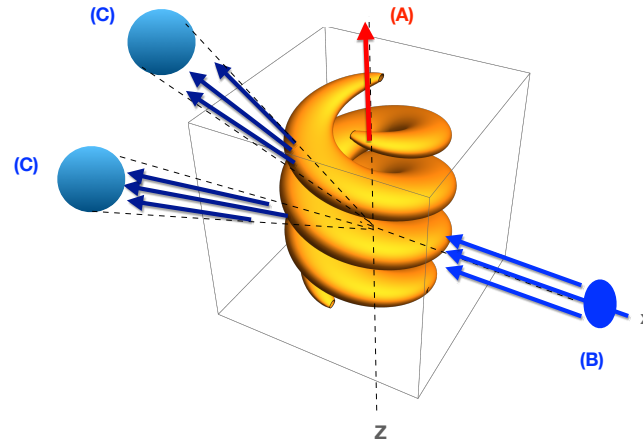


Figure 1. Geometry of Penrose scattering in vacuum: (A)—an intense light spring propagates in the z direction, with frequencies ω_1 and ω_2 , its intensity rotates around the z axis; (B) a probe pulse with frequency ω_i propagates along the (negative) x direction and collides perpendicularly with the light spring; (C) scattered signals are emitted with frequencies ω_{\pm} and an angular spread dictated by the light spring structure.

We describe quantum vacuum using the lowest order Euler–Heisenberg Lagrangian [11]. This is valid for field amplitudes that stay constant on a time scale much longer than the Compton time, $\tau_C = h/m_e c^2 \simeq 1.3 \times 10^{-21}$ s, and amplitudes that are well below the Schwinger limit, $E_S = m_e^2 c^3 / \hbar e \simeq 10^{16}$ V/cm, when real e-p pairs are absent, and QED vacuum effects are dominated by virtual pairs. This is the appropriate regime for possible experiments with the existing high-intensity laser systems.

In this approach, the electromagnetic vacuum response is determined by the polarization and magnetization vectors, \mathbf{P} and \mathbf{M} , which are given by the two symmetric expressions

$$\mathbf{P} = -2\zeta(4\mathcal{F}\mathbf{E} - 7c\mathcal{G}\mathbf{B}), \quad \mathbf{M} = -2\zeta c^2(4\mathcal{F}\mathbf{B} + 7c\mathcal{G}\mathbf{E}/c). \quad (7)$$

Here, \mathbf{E} and \mathbf{B} are the electric and magnetic field amplitudes, and \mathcal{F} and \mathcal{G} are the two invariant quantities

$$\mathcal{F} = \frac{1}{2}(c^2 B^2 - E^2), \quad \mathcal{G} = c(\mathbf{E} \cdot \mathbf{B}). \quad (8)$$

We have also used the nonlinear quantum parameter ζ , which determines the strength of the quantum vacuum nonlinearity, which is defined as

$$\zeta = 2\alpha^2 \frac{\epsilon_0^2 \hbar^3}{45m^4 c^5}, \quad \alpha = \frac{e^2}{2\epsilon_0 \hbar c}, \quad (9)$$

where $\epsilon_0 = 1/c^2 \mu_0$ is the vacuum permittivity, $\hbar = h/2\pi$ is Planck’s constant divided by 2π , m is the electron mass, and $\alpha \simeq 1/137$ is the fine structure constant. As already mentioned, such a description is valid for weak fields, $E \ll E_S$, where the Schwinger field

is $E_S = m^2 c^3 / e \hbar \simeq 1.32 \times 10^{18}$ V/m. In order to describe the properties of the scattered signal, we use the wave equation valid for a disturbed quantum vacuum, of the form

$$\left(\nabla^2 - \frac{1}{c^2} \frac{\partial^2}{\partial t^2} \right) \mathbf{E} = \mu_0 \left[\frac{\partial \mathbf{J}}{\partial t} + c^2 \nabla (\nabla \cdot \mathbf{P}) \right], \quad (10)$$

where the nonlinear current \mathbf{J} is

$$\mathbf{J} = \frac{\partial \mathbf{P}}{\partial t} + \nabla \times \mathbf{M}, \quad (11)$$

In the next section, we calculate the currents responsible for the emission of scattered radiation.

3. Quantum Currents

Let us then assume an incident probe field propagating in the perpendicular direction, as described by

$$\mathbf{E}_i(\mathbf{r}, t) = \mathbf{E}_i \exp(i\mathbf{k}_i \cdot \mathbf{r} - i\omega_i t), \quad (12)$$

where $\mathbf{k}_i = -k_i \mathbf{e}_x$ (see Figure 1). If we ignore nonlinear dispersion corrections due to the light spring, we can write $k_i = \omega_i / c$. Our aim is to calculate the field scattered by the rotating nonlinear structure described by the field \mathbf{E}_0 , defined in Equation (1). The total field of our problem can therefore be written as

$$\mathbf{E} = \mathbf{E}_0 + \mathbf{E}_i + \mathbf{E}_s, \quad \mathbf{B} = \mathbf{B}_0 + \mathbf{B}_i + \mathbf{B}_s, \quad (13)$$

where \mathbf{E}_i and \mathbf{B}_i are the probe fields, and \mathbf{E}_s and \mathbf{B}_s are the second-order scattered fields. Notice that the magnetic field associated with the light spring is given by

$$\mathbf{B}_0(\mathbf{r}, t) = \sum_{\nu=1,2} \mathbf{B}_\nu F_\nu(r, \theta) \exp(i\mathbf{k}_\nu \cdot \mathbf{z} - i\omega_\nu t) + c.c., \quad (14)$$

where

$$\mathbf{B}_\nu = \frac{E_\nu}{c} \left[\left(\frac{\mathbf{k}_\nu c}{\omega_\nu} \times \mathbf{e}_\nu \right) + \left(\frac{i\ell_\nu}{r} \mathbf{e}_r + \frac{1}{F_\nu} \frac{\partial F_\nu}{\partial r} \mathbf{e}_\theta \right) \right]. \quad (15)$$

In the particular case of $\mathbf{k}_\nu = k_\nu \mathbf{e}_z$ mentioned earlier, and assuming that the two light spring components are linearly polarized at an angle θ_ν relative the the x axis, we obtain

$$\left(\frac{\mathbf{k}_\nu c}{\omega_\nu} \times \mathbf{e}_\nu \right) = -\mathbf{e}_\theta. \quad (16)$$

According to Equations (10) and (13), the wave equation for the scattered radiation is given by

$$\left(\nabla^2 - \frac{1}{c^2} \frac{\partial^2}{\partial t^2} \right) \mathbf{E}_s = \mu_0 \left[\frac{\partial \mathbf{J}_s}{\partial t} + c^2 \nabla (\nabla \cdot \mathbf{P}_s) \right], \quad (17)$$

where the source terms are independent of the second-order fields and are therefore $\mathbf{J}_s \equiv \mathbf{J}_s(\mathbf{E}_\nu, \mathbf{E}_i)$ and $\mathbf{P}_s \equiv \mathbf{P}_s(\mathbf{E}_\nu, \mathbf{E}_i)$. In order to calculate these terms, we start with the invariants (8). They can be approximately written as

$$\mathcal{F}_s = \frac{1}{2} \sum_\nu \left(c^2 \mathbf{B}_\nu^* \cdot \mathbf{B}_i - \mathbf{E}_\nu^* \cdot \mathbf{E}_i \right) F_\nu(r) \exp(i\varphi_\nu) + c.c., \quad (18)$$

and

$$\mathcal{G}_s = c \sum_\nu \left(\mathbf{E}_\nu^* \cdot \mathbf{B}_i + \mathbf{E}_i \cdot \mathbf{B}_\nu^* \right) F_\nu(r) \exp(i\varphi_\nu) + c.c., \quad (19)$$

with the phase

$$\varphi_\nu = -\ell_\nu \theta + (\mathbf{k}_i - \mathbf{k}_\nu) \cdot \mathbf{r} - (\omega_i - \omega_\nu) t. \quad (20)$$

In these expressions, we have used the equality $(c^2B_i^2 - E_i^2) = 0$. We also assumed that $(c^2B_v^2 - E_v^2) \simeq 0$, which corresponds to neglecting the second term in Equation (15). This term would lead to corrections of order $1/k_v w$, where w is the beam waist, which are assumed to be much smaller than one. Notice that in the above expressions, the other neglected contributions are second-order corrections to the dispersion relation of the scattered field. These simplifying assumptions do not significantly contribute to the final result.

The above invariants can be used to calculate the quantities \mathbf{J}_s and \mathbf{P}_s , where only terms of the form $(E_v^* E_v E_i)$ contribute to the scattered radiation for frequencies determined by $\omega_{\pm} = (\omega_i \pm \Delta\omega)$, as shown next. We first write the nonlinear polarization \mathbf{P}_s and magnetization \mathbf{M}_s as

$$\mathbf{P}_s = -2\zeta(4\mathcal{F}_s \mathbf{E}_0 - 7c\mathcal{G}_s \mathbf{B}_0), \quad \mathbf{M}_s = -2c\zeta(4c\mathcal{F}_s \mathbf{B}_0 + 7\mathcal{G}_s \mathbf{E}_0). \quad (21)$$

After a straightforward calculation, we obtain

$$\mathbf{P}_s = -2\zeta \sum_{v,v'} \mathbf{p}_s(E_v^* E_v E_i) F_v F_{v'} \exp(i\varphi'_s). \quad (22)$$

and

$$\mathbf{M}_s = -2c\zeta \sum_{v,v'} \mathbf{m}_s(E_v^* E_v B_i) F_v F_{v'} \exp(i\varphi_{vv'}). \quad (23)$$

where we have used the auxiliary phase functions

$$\varphi_{vv'} = (\ell_v - \ell_{v'})\theta + (\mathbf{k}_i - \mathbf{k}_v + \mathbf{k}_{v'}) \cdot \mathbf{r} - (\omega_i - \omega_v + \omega_{v'})t, \quad (24)$$

and the auxiliary polarization and magnetization vectors

$$\mathbf{p}_s = 2(\mathbf{b}_v^* \cdot \mathbf{b}_i - \mathbf{e}_v \cdot \mathbf{e}_i) \mathbf{e}_{v'} - 7(\mathbf{e}_v^* \cdot \mathbf{e}_i + \mathbf{b}_v^* \cdot \mathbf{e}_i) \mathbf{b}_{v'}, \quad (25)$$

and

$$\mathbf{m}_s = 2(\mathbf{b}_v^* \cdot \mathbf{b}_i - \mathbf{e}_v \cdot \mathbf{e}_i) \mathbf{b}_{v'} + 7(\mathbf{e}_v^* \cdot \mathbf{e}_i + \mathbf{b}_v^* \cdot \mathbf{e}_i) \mathbf{e}_{v'}, \quad (26)$$

The unit vectors $\mathbf{e} = \mathbf{E}/|E|$ and $\mathbf{b} = \mathbf{B}/|B|$, with appropriate subscripts, were also used. Of particular interest is the case considered here, where the two components of the light spring propagate along the z -axis, with $\mathbf{k}_v = k_v \mathbf{e}_z$, and the probe propagates along the x -axis, in the negative direction, with $\mathbf{k}_i = -k_i \mathbf{e}_x$. To simplify, we also use $\mathbf{e}_v = \mathbf{e}_x$. In this case, we can write the auxiliary polarization vectors in a much simpler form as

$$\mathbf{p}_s = 2(\mathbf{b}_v^* \cdot \mathbf{b}_i) \mathbf{e}_{v'} - 7(\mathbf{b}_v^* \cdot \mathbf{e}_i) \mathbf{b}_{v'}, \quad (27)$$

This allows us to write the nonlinear current as $\mathbf{J}_s = \mathbf{J}_0 + \mathbf{J}_{\pm}$, where the first term corresponds to $v = v'$. Notice that \mathbf{J}_0 only contributes to elastic scattering, because it evolves in space and time according to the phase φ_i . Elastic scattering is an interesting process, which can be associated with vacuum birefringence and has been discussed in the literature [26]. Here, we focus on the inelastic scattering term \mathbf{J}_{\pm} , that is associated with a frequency shift and a different direction of propagation. This could be more favorable for detection. We can write this term as

$$\mathbf{J}_{\pm} = 2iR_{12}(r)\zeta|E_1 E_2| E_i \sum_{\pm} \omega_{\pm} \mathbf{j}_{\pm} \exp(i\varphi_{\pm}), \quad (28)$$

where $R_{12}(r) = F_1(r)F_2(r)$ determines the radial structure, $\omega_{\pm} = \omega_i \pm \Delta\omega$ are the emitted frequencies, and the phase functions become

$$\varphi_{\pm} = \pm\Delta\ell\theta + \mathbf{k}_{\pm} \cdot \mathbf{r} - \omega_{\pm}t, \quad (29)$$

with $\mathbf{k}_\pm = (\mathbf{k}_i \pm \Delta\mathbf{k})$. Finally, we have used the auxiliary current vector

$$\mathbf{j}_\pm = \mathbf{p}_s + \left(\frac{\mathbf{k}_\pm c}{\omega_\pm} \times \mathbf{m}_\pm \right) \tag{30}$$

where \mathbf{m}_\pm is defined below, $\mathbf{p}_+ = \mathbf{p}_s(\nu = 1, \nu' = 2)$ and $\mathbf{p}_- = \mathbf{p}_s(\nu = 2, \nu' = 1)$. Similarly, for the nonlinear magnetization, we have $\mathbf{M}_s = \mathbf{M}_0 + \mathbf{M}_\pm$, where the terms contributing to inelastic scattering are

$$\mathbf{M}_\pm = -2cR_{12}(r)\zeta|E_1E_2|B_i \sum_{\pm} \mathbf{m}_\pm \exp(i\varphi_\pm), \tag{31}$$

with

$$\mathbf{m}_+ = 2(\mathbf{b}_1^* \cdot \mathbf{b}_i)\mathbf{b}_2 + 7(\mathbf{b}_1^* \cdot \mathbf{e}_i)\mathbf{e}_2, \tag{32}$$

and \mathbf{m}_- is obtained by interchanging the subscripts 1 and 2. Notice that the quantities \mathbf{J}_0 and \mathbf{M}_0 only give negligible nonlinear corrections to the refractive index of the incident wave at frequency ω_i . Although they are not explicitly written, because they are not relevant to inelastic scattering, they are of the same order of magnitude as \mathbf{J}_\pm and \mathbf{M}_\pm .

4. Scattered Radiation

Let us now go back to the wave equation for the scattered field, Equation (17), and search for a solution of the form

$$\mathbf{E}_s(\mathbf{r}, t) = \mathbf{E}_s(\mathbf{r}, \omega) \exp(-i\omega t). \tag{33}$$

The quantity $\mathbf{E}_s(\mathbf{r}, \omega_\pm)$ is a solution of

$$\left(\nabla^2 + \frac{\omega^2}{c^2} \right) \mathbf{E}_s(\mathbf{r}; \omega) = -i\mu_0 \int \omega \mathbf{J}_s(\mathbf{r}; \omega) \exp(i\omega t) dt, \tag{34}$$

Here, we only retain the dominant term (for a detailed discussion, see [27]). Using Equation (28), we can write

$$\left(\nabla^2 + \frac{\omega^2}{c^2} \right) \mathbf{E}_s(\mathbf{r}; \omega) = 2\omega\mu_0 R_{12}(r)\zeta|E_1E_2|E_i \mathcal{I}_\omega, \tag{35}$$

with the integral

$$\mathcal{I}_\omega = \int \omega_\pm \mathbf{j}_\pm \exp(i\varphi_\pm) dt, \tag{36}$$

From here, we can easily obtain

$$\mathcal{I}_\omega = 2\pi\omega_\pm \mathbf{j}_\pm \delta(\omega - \omega_\pm) e^{i\pm\Delta\ell\theta} e^{i\mathbf{k}_\pm \cdot \mathbf{r}}, \tag{37}$$

Noting that the scattered field in Equation (35) has to satisfy the vacuum dispersion relation $k = \omega/c$, we can write for the field amplitude

$$E_s(\mathbf{r}, \omega) = \frac{2\omega^2}{k} \mu_0 \zeta |E_1 E_2| E_i (\mathbf{e}_s^* \cdot \mathbf{j}_\pm) \mathcal{I}(\mathbf{r}) e^{i\mathbf{k} \cdot \mathbf{r}}, \tag{38}$$

with the new integral

$$\mathcal{I}(\mathbf{r}) = \int^{\mathbf{r}} R_{12}(r') e^{\pm i\Delta\ell\theta} e^{i(\mathbf{k}_\pm - \mathbf{k}) \cdot \mathbf{r}'} d\mathbf{r}', \tag{39}$$

where \mathbf{e}_s is the unit polarization vector of the scattered field. At this point, it is important to note that the wavevector \mathbf{k} is not identical to \mathbf{k}_\pm , because it has to satisfy the vacuum dispersion relation $k = \omega/c$. In contrast, the frequency of the scattering radiation is exactly defined by $\omega = \omega_\pm \equiv \omega_i \pm \Delta\omega$. This leads to the relation $k^2 = (k_i \pm \Delta k)^2$. On the other

hand, given that \mathbf{k}_i and $\Delta\mathbf{k}$ are orthogonal, we immediately have $k_{\pm}^2 = k_i^2 \pm \Delta k^2$ and we conclude that $\mathbf{k} \neq \mathbf{k}_{\pm}$.

Therefore, due to momentum conservation, the scattered radiation receives an additional amount of momentum, which is coming from the light spring structure described by $R_{12}(r)$. This is an important aspect of the present scattering mechanism. To understand it properly, we define $\mathbf{k} = -k_i\mathbf{e}_x \pm \Delta k\mathbf{e}_z + \mathbf{q}$, and assume that the additional amount of momentum is in the x direction: $\mathbf{q} = -q_x\mathbf{e}_x$. Replacing this in Equation (39), and integrating in z , we obtain

$$\mathcal{I}(\mathbf{r}) = 2\pi \int^{\mathbf{r}_{\perp}} R_{12}(r') e^{\pm i\Delta\ell\theta + iq_x x'} d\mathbf{r}'_{\perp}, \tag{40}$$

where $d\mathbf{r}'_{\perp} = r dr d\theta$. From here, we can easily obtain

$$\mathcal{I}(\mathbf{r}) = (2\pi)^2 \sum_{\ell'} w' J_{\ell'}(q_x w') \delta(\ell' \pm \Delta\ell), \tag{41}$$

where $J_{\ell'}$ are Bessel functions of the first kind. The quantity w' in this expression is nearly equal to the light spring spot-size w , and it is more exactly defined by the equality

$$w' J_{\ell'}(q_x w') = \int_0^{\infty} R_{12}(r) J_{\ell'}(q_x r) r dr. \tag{42}$$

We see that this quantity is of order one, as illustrated in Figure 2. As a final step of our calculation, we arrive at an expression for the scattered field amplitude of the form

$$E_s(\mathbf{r}, \omega) = 2^3 \pi a_0^2 E_i \mathcal{R} \frac{\omega_2}{\omega_1} (\mathbf{e}_s^* \cdot \mathbf{j}_{\pm}) \sum_{\ell'} (k w') J_{\ell'}(q_x w') \delta(\ell' \pm \Delta\ell), \tag{43}$$

where $a_0 = eE_0/mc\omega_1$ is the dimensionless field amplitude of the intense light spring, and $E_1 = E_2 = E_0$ is assumed, and the quantity \mathcal{R} is the fundamental nonlinear parameter of vacuum introduced in [27]. It is defined as

$$\mathcal{R} = \frac{\alpha}{45} \left(\frac{\hbar\omega_1}{mc^2} \right)^2, \tag{44}$$

where α is the fine structure constant. Similarly, we can consider the case of the scattered radiation with a small y component. For this purpose, we now use $q_x = 0$ and assume that $\mathbf{q} = q_y\mathbf{e}_y$. This leads to a similar expression for the scattered field, where the quantity $J_{\ell'}(q_x w') \delta(\ell' \pm \Delta\ell)$ is replaced by $J_{\ell'}(q_y w') (i)^{\ell'} \delta(\ell' \mp \Delta\ell)$.

We arrive at the conclusion that the scattered radiation, with frequency $\omega = \omega_{\pm}$, spreads with nearly equal amplitude over a spot size of order w' around the direction defined by the wavevector \mathbf{k}_{\pm} in both the x and the y -directions. This is due to the additional amount of momentum imparted by the light spring structure. This additional amount of momentum \mathbf{q} is always of order $\Delta\mathbf{k}$. The resulting scattered field amplitude can then be written, in order of magnitude, as

$$\frac{|E_s|}{E_i} \simeq 2^3 \pi (k w) \frac{\alpha}{45} a_0^2 \left(\frac{\hbar\omega_1}{mc^2} \right)^2 \frac{\omega_2}{\omega_1}. \tag{45}$$

We notice the numerical factor $2\pi(\alpha/45) \sim 10^{-3}$. This amplitude is essentially determined by the intensity of the light spring a_0^2 and by the initial photon frequencies $\omega_{1,2}$. It is actually of the same order of magnitude as that of other wave-mixing processes resulting from photon–photon scattering in vacuum, which is no surprise. The main advantage of the present configuration is that the frequency of the scattered field can be very different from the incident frequency, $\omega \neq \omega_i$. In the same way, the direction of propagation, $\mathbf{k} \neq \mathbf{k}_i$, could provide a good experimental geometry. But the more interesting property of the present scattering configuration is that the scattering direction is not only determined by the wave vectors of the interacting waves but also the helical nature of

the nonlinear object. Therefore, it provides a new and somewhat unexpected vacuum configuration for what can be considered an analogue of the Penrose scattering.

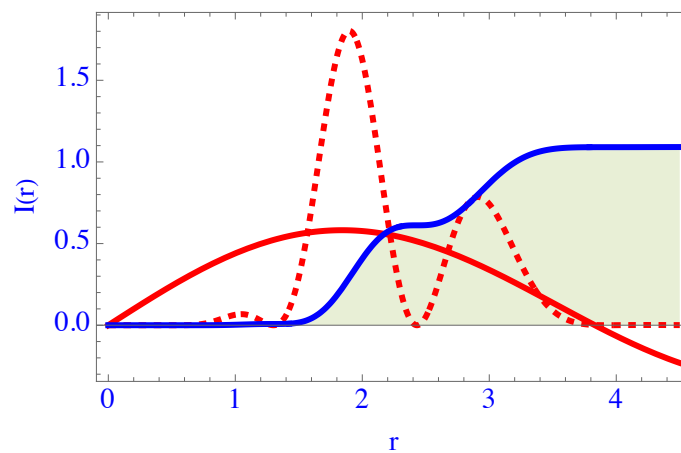


Figure 2. Representation of the radial integral $\mathcal{I}(r)$, for $\Delta\ell = 1$, with $J_1(r)$ in red, $R_{12}(r)$ in dashed red. We have used $\ell_1 = 14$ and $k = 1$.

5. Conclusions

In this work, we have considered a new mechanism of photon–photon scattering in a quantum vacuum, which is inspired in the Penrose scattering process. In our model, the scatterer is not a black hole but a rotating object made of purely electromagnetic radiation with orbital angular momentum (OAM), which propagates in vacuum as a light spring. This electromagnetic object is made of two twisted modes with different frequencies ω_1 and ω_2 and different helicity states, ℓ_1 and ℓ_2 . In recent years, intense laser beams have been produced experimentally at the peta-watt intensity level, and the use of light springs at these intensities is therefore conceivable [28,29]. It is also conceivable that the use of peta-watt light springs, with intensity $a_0^2 \gg 1$ such that it compensates the small vacuum parameter R in Equation (44), will bring the scattered field E_s to a detectional level.

An incident probe pulse, with frequency ω_i , is scattered in two different directions, which are determined by the light spring structure. As expected, the photon–photon coupling efficiency associated with this new scattering process is not different from that of the already known configurations [7,27]. However, it could represent some experimental interest, because of the two symmetric frequency shifts, for signals propagating in two symmetrically oriented scattered directions. This is important because it could improve the signal-to-noise ratio, which imposes severe constraints in these kinds of experiments. In our approach, the probe beam was described as a plane wave to simplify the equations. But extension to a focused laser probe (for instance, a Gaussian laser beam) is straightforward, using a standard Fourier analysis of the incident and scattered signals.

It should be added that the present model, although directly inspired by the Penrose process of light scattering by a rotating black hole, is only partly related to this process. In particular, we were not able to demonstrate the amplification of the incident signal, the so-called Zel’dovich–Misner effect, which is a characteristic feature of the original model. Here, we observe total energy conservation, which is typical of a nonlinear wave mixing process. It is true that in previous nonlinear optics experiments [19,30], the same wave mixing processes are operating but in a distinct physical configuration. The observed amplification results from superfluid light phenomena (diffraction effects) that can occur inside the pump beam and are ignored here.

Funding: This research received no external funding.

Data Availability Statement: Data are contained with the article.

Acknowledgments: The author would like to thank Gert Brodin for stimulating discussions on laser QED problems, during a short visit to Umeå University.

Conflicts of Interest: The author declares no conflicts of interest.

References

1. Yoon, J.W.; Kim, Y.G.; Choi, I.W.; Sung, J.H.; Lee, H.W.; S.K. Lee, S.K.; C.H. Nam, C.H. Realization of Laser Intensity over 10^{23} W/cm². *Optica* **2021**, *8*, 630.
2. Di Piazza, A.; Müller, C.; Hatsagortsyan, K.Z.; Keitel, C.H. Extremely High-Intensity Laser Interactions with Fundamental Quantum Systems. *Rev. Mod. Phys.* **2012**, *84*, 1177.
3. Gonoskov, A.; Blackburn, T.G.; Marklund, M.; Bulanov, S.S. Charged Particle Motion and Radiation in Strong Electromagnetic Fields. *Rev. Mod. Phys.* **2022**, *94*, 045001.
4. Fedotov, A.; Ilderton, A.; Karbstein, F.; King, B.; Seipt, D.; Taya, T.; G. Torgrimsson, G. Advances in QED with Intense Background Fields. *Phys. Rep.* **2023**, *1010*, 1–138.
5. Brodin, G.; Marklund, M.; Stenflo, L. Proposal for Detection of QED Vacuum Nonlinearities in Maxwell's Equations by the Use of Waveguides. *Phys. Rev. Lett.* **2001**, *87*, 171801.
6. Bialynicka-Birula, Z.; Bialynicki-Birula, I. Nonlinear Effects in Quantum Electrodynamics. Photon Propagation and Photon Splitting in an External Field. *Phys. Rev. D* **1970**, *2*, 2341.
7. Lundstrom, E.; Brodin, G.; Lundin, J.; Marklund, M.; Bingham, R.; Collier, J.; Mendonça, J.T.; Norreys, P. Using High-Power Lasers for Detection of Elastic Photon-Photon Scattering. *Phys. Rev. Lett.* **2006**, *96*, 083602.
8. Gies, H.; Karbstein, F.; Seegert, N. Quantum Reflection of Photons off Spatio-temporal Electromagnetic Field Inhomogeneities. *New J. Phys.* **2015**, *17*, 043060.
9. Mendonça, J.T.; Marklund, M.; Shukla, P.K.; Brodin, G. Photon Acceleration in Vacuum. *Phys. Lett. A* **2006**, *359*, 700.
10. Schwinger, J. On Gauge Invariance and Vacuum Polarization. *Phys. Rev.* **1951**, *82*, 664.
11. Heisenberg, W.; Euler, H. Consequences of Dirac's Theory of Positrons. *Z. Phys.* **1936**, *98*, 714.
12. Gies, H.; Karbstein, F. An Addendum to the Heisenberg-Euler Effective Action Beyond One Loop. *J. High Energy Phys.* **2017**, *03*, 108.
13. Mendonça, J.T. Superradiance in Quantum Vacuum. *Quantum Rep.* **2021**, *3*, 42.
14. Mendonça, J.T. Particle-Pair Creation by High-Harmonic Laser Fields. *Phys. Scr.* **2023**, *98*, 125606.
15. Penrose, R. Gravitational Collapse: The Role of General Relativity. *Gen. Rel. Grav.* **2002**, *34*, 1141; *Riv. Nuovo Cim.* **1969**, *1*, 252.
16. Zel'dovich, Y.B. Amplification of Cylindrical Electromagnetic Waves Reflected from a Rotating Body. *Sov. J. Exp. Theor. Phys.* **1972**, *35*, 1085.
17. Brito, R.; Cardoso, V.; Pani, P. *Superradiance*; Springer: Cham, Switzerland, 2020; Volume 906, 1–237.
18. Zhang, H.; Zhang, B. Shielding of Penrose Superradiance in Optical Black Holes. *Eur. Phys. J. C* **2023**, *83*, 233.
19. Braidotti, M.C.; Prizia, R.; Maitland, C.; Marino, F.; Prain, A.; Starshynov, I.; Westerberg, N.; Wright, E.M.; Faccio, D. Measurement of Penrose Superradiance in a Photon Superfluid. *Phys. Rev. Lett.* **2022**, *128*, 013901.
20. Cromb, M.; Gibson, G.M.; Toninelli, E.; Padgett, M.J.; Wright, E.M.; Faccio, D. Amplification of Waves from a Rotating Body. *Nat. Phys.* **2020**, *16*, 1069.
21. Torres, T.; Patrick, S.; Coutant, A.; Richartz, M.; Tedford, E.W.; Weinfurter, S. Rotational Superradiant Scattering in a Vortex Flow. *Nat. Phys.* **2017**, *13*, 833.
22. Mendonça, J.T.; Vieira, J.; Willim, C.; Fedele, R. Particle Acceleration by Twisted Laser Beams. *Front. Phys.* **2022**, *10*, 995379.
23. Vieira, J.; Mendonça, J.T.; Quéré, F. Optical Control of the Topology of Laser-Plasma Accelerators. *Phys. Rev. Lett.* **2018**, *121*, 054801.
24. Mendonça, J.T.; Willim, C.; Vieira, J. Twisted Waves near a Plasma Cutoff. *Symmetry* **2022**, *14*, 146.
25. Pariente, G.; Quéré, F. Spatio-Temporal Light Springs: Extended Encoding of Orbital Angular Momentum in Ultrashort Pulses. *Opt. Lett.* **2015**, *40*, 2037.
26. Karbstein, F.; Gies, H.; Reuter, M.; Zepf, M. Vacuum birefringence in strong inhomogeneous electromagnetic fields. *Phys. Rev. D* **20115**, *92*, 071301(R).
27. Mendonça, J.T. Emission of Twisted Photons from Quantum Vacuum. *EuroPhys. Lett.* **2017**, *120*, 61001.
28. Li, S.; Li, G.; Ain, Q.; Hur, M.S.; Ting, A.C.; Kulagin, V.V.; Kamperidis, C.; Hafz, N.A.M. A laser-plasma accelerator driven by two-color relativistic femtosecond laser pulses. *Sci. Adv.* **2019**, *5*, eaav7940.
29. Wang, J.W.; Zepf, M.; Rykovanov, S.G. Intense Attosecond Pulses Carrying Orbital Angular Momentum using Laser Plasma Interactions. *Nat. Commun.* **2019**, *10*, 5554.
30. Braidotti, M.C.; Marino, F.; Wright, E.M.; Faccio, D. The Penrose Process in Nonlinear Optics. *AVS Quantum Sci.* **2022**, *4*, 010501.

Disclaimer/Publisher's Note: The statements, opinions and data contained in all publications are solely those of the individual author(s) and contributor(s) and not of MDPI and/or the editor(s). MDPI and/or the editor(s) disclaim responsibility for any injury to people or property resulting from any ideas, methods, instructions or products referred to in the content.